

A host-pathogen simulation model: powdery mildew of grapevine

A. Calonnec^{a*}, P. Cartolaro^a, J.-M. Naulin^a, D. Bailey^{a†} and M. Langlais^b

^aINRA-Bordeaux, UMR INRA-ENITA 1065 Santé Végétale BP 81, 33883 Villenave d'Ornon; and ^bUMR CNRS 5251, IMB & INRIA Futurs Anubis case 26, Université Victor Segalen Bordeaux 2, 33076 Bordeaux, France

An epidemiological model simulating the growth of a single grapevine stock coupled to the dispersal and disease dynamics of the airborne conidia of the powdery mildew pathogen *Erysiphe necator* was developed. The model input variables were either climatic (temperature, wind speed and direction) or related to the pathogen (location and onset of primary infection). The environmental input variables dictated plant growth and pathogen spread (latent period, infection, lesion growth, conidial spore production and release). Input parameters characterized the crop production system, the growth conditions and the epidemiological characteristics of the pathogen. Output described, at each time step, number, age and pattern of healthy and infected organs, infected and infectious leaf area and aerial density of spores released. Validation of the model was achieved by comparing model output with experimental data for epidemics initiated at different times of host growth. Epidemic behaviour for two contrasting years of crop development and 7 phenological stages at the time of primary infection (PI) was examined. For PI occurring at day 115 a vine with late budbreak (1998) showed 58% of primary leaves diseased at flowering compared with only 19% for a vine with early budbreak (2003). Depending on the phenological stage at PI (1–4 leaves), the proportion of diseased primary leaves decreased from 42% to 6% at flowering. Simulations suggested that differences resulted from the interplay between the timing of the first sporulation event, the phenological stage at the time of initial infection, and the age structure and spatial distribution of the leaf population.

Keywords: architectural model, dispersal, *Erysiphe necator*, invasive spread, *Vitis vinifera*

Introduction

In this paper the construction of a detailed, discrete deterministic simulation model coupling the development and spread of a fungus *Erysiphe necator*, with the development of its host, the perennial crop *Vitis vinifera*, is described. The model was used to show, by simulation, the dependence of epidemic development on climatic variables and crop management parameters. The model was designed to (i) quantify and rank the most important host and pathogen factors that modify the dynamic interactions between pathogen, host and their environment and, (ii) simulate the spatiotemporal dynamics of host growth and epidemic development, beginning from a range of climatic conditions, production systems and initial conditions for the density and location of the pathogen, in order to identify situations most conducive to the spread of disease.

The grape-powdery mildew pathosystem is characterized by a polycyclic pathogen capable of explosive multiplication and a host population with a high degree of spatial structure at the field level and with a complex architecture of leaf and berry structure at the individual plant level exhibiting rapid changes over time. As well as environmental differences, the high degree of human interference during vine development and the wide diversity of cropping systems further enhances variability from one crop to another and hence, variability between epidemics. Primary infection occurs either through ascospore release from chasmothecia that overwinter in the bark of the vine (Cortesi *et al.*, 1995) or via colonization of new shoots from resting mycelium that overwinter within dormant buds (Sall & Wrysinski, 1982). Epidemics continue to spread by secondary infections by conidia from sporulating lesions of infected leaves to new susceptible leaves. Importantly, the leaf epidemic provides a source of inoculum for the infection of developing berries. Because of the tight relationship between powdery mildew and its host (Doster & Schnathorst, 1985; Ficke *et al.*, 2002, 2003; Gadoury *et al.*, 2003) and of the spatial location of primary infections on the vine stock, dynamic changes in crop structure should be considered as key factors for explaining variability in the severity of epidemic behaviour.

*E-mail: calonnec@bordeaux.inra.fr

†Present address: UMR Bio3P, INRA-Agrocampus Rennes, BP35327, 35653 Le Rheu cedex, France.

Accepted 20 August 2007

Indeed, by modifying the movement of inoculum (by creating a leaf barrier or by altering the distance between infected and susceptible leaves), or by altering the susceptibility of the leaf population as it changes with age of the crop, natural and management-induced changes in crop growth and crop architecture may significantly affect the course of an epidemic.

In the first analytical model of Van der Plank (1963, 1982) disease development was proportional to the amount of infectious (sporulating) and available tissue with a constant infection rate (multiplication factor of disease per unit), a constant latent period and with random dispersion of inoculum between infected and susceptible hosts. There have been several attempts to combine host and pathogen development since in order to account for the effect of changing environments on disease progress. According to Hau (1990), the only way for a disease progress curve to diminish is through a changing host, either by (i) an increase of susceptible tissue, referred to as a dilution effect, or (ii) by the loss of the diseased tissue by defoliation, referred to as a thinning-out effect, or (iii) as a result of ontogenic resistance. For vine and powdery mildew, a set of deterministic models taking into account host growth and based on the modified Van der Plank equations were developed (Sall, 1980; Blaise & Gessler, 1992; Gessler & Blaise, 1992). In the Sall model, vine growth was introduced through a submodel of global surface area evolving as a function of temperature and time. The apparent infection rate was a function of temperature and moisture. The model was able to describe differences in disease severity depending on weather conditions, especially temperature. Blaise & Gessler (1992), introduced host growth into Van der Plank's equation as a homogenous, increasing susceptible surface, and a latent period as a function of temperature. In their simulations, introduction of host growth affected the rate of infection and was sufficient to slow down or even arrest the spread of disease. The model did not, however, account for studies concerning the dependence of infection rate on pathogen dispersal and/or on host-pathogen interactions. The infection rate used to initiate the model was calculated from epidemic data, incorporating environmental conditions of that epidemic alone. Thus, for a better understanding of host/pathogen dynamic interactions and the capacity of host development to modify disease progress, a spatially explicit, epidemiological simulation model coupling vine stock growth with the spread of powdery mildew was developed in the present work. This model incorporated terms for the dynamics of host growth, ontogenic resistance, the distance between susceptible and resistant organs, the synchronism between host and pathogen development, and the epidemiological traits of pathogen growth and dispersal. The model was built at the scale of a single vine, yet facilitated the study of interactions between all of these components during a single growing season. The behaviour of the model and the interactions at the single-vine scale was considered an essential first step prior to incorporating the role of the host, i.e. crop structure and heterogeneity in vine vigour,

into powdery mildew invasion at larger scale (Calonnec *et al.*, 2005; Tessier *et al.*, 2006). Because of the complexity involved in the accurate description of the geometry of cluster development (Fanizza & Colonna, 1996) and the high correlation between damage on bunches and the amount and dynamics of the disease on leaves, the spread of disease was restricted to the leaf population only. Indeed, the spatial relationship between the maps of the frequency of diseased leaves around flowering and the maps of frequency of bunches with high severity at bunch closure was demonstrated on grape cv. Cabernet Sauvignon (Peyrard *et al.*, 2005; Calonnec *et al.*, 2006). The development of the spatial arrangement of host organs within the vine stock was achieved by using a 3-D architectural model. Such virtual plant growth models providing visual output already exist (Weber & Penn, 1995; Deussen & Linterman, 1997; Prusinkiewicz, 1997) and are considered powerful research tools (Room *et al.*, 1996; Birch *et al.*, 2003), especially after interfacing with models of plant ecophysiology (Tardieu, 2003), insect behaviour (Hanan *et al.*, 2002; Skirvin, 2006) or disease damage (Wilson & Chakraborty, 1998).

In this paper the derivation, parameterization, output and behaviour of the epidemiological model coupling the temporal and spatial vine growth with the development and spread of powdery mildew at the vine stock scale is presented. To illustrate the behaviour of the model and the use of the model as a research tool, epidemics were simulated using environmental data reflecting two contrasting but representative seasons of vine growth. The model was used to identify key processes in the interplay between host and pathogen factors that account for differences in epidemic development.

Materials and methods

Model derivation

The model simulated the development of a single vine stock during a single season. This was coupled with the simulation of inoculum and disease dynamics from primary infection of susceptible leaves and secondary conidial infection as disease spreads from sporulating lesions. Functions, parameterized from the literature or from experimental data, were used to describe growth of the host and spread of the pathogen. The model input variables were environmental (temperature, wind speed and direction) or related to the pathogen (location and onset of primary infection). The environmental input variables dictated growth of the crop (appearance and growth of organs) and spread of the pathogen (latent period, infection, lesion growth, spore production and release). Input parameters characterized the crop system (number of buds, training system) and conditions of growth for the vine and the pathogen.

Grapevine development

The development of the spatial arrangement of host organs within the vine stock was captured within a 3-D

architectural model. An object-based approach, considering the plant as a structure composed of relatively simple units (leaves, internodes, growth units, etc.), was used. This had the advantage that changes in plant architecture would appear automatically in the model, resulting from interactions between the units. The generation rules were derived from the following assumptions:

(i) Plants naturally involve, not just a set of elements, but also a set of connections between pairs of elements. To model this situation, abstract objects called graphs (a graph being a set of vertices and a set of edges that connect pairs of distinct vertices) (West, 1995; Diestel, 2000) were used. The vine stock was divided into three principal components: leaves, internodes and bunches. Each element was connected to subsequent elements by order of growth and could be tracked in space by its x, y and z coordinates, which could, in turn, be used to store all other associated information (e.g. position, angle, age, etc.). This relatively simple structure enabled the state of the plant and of each of its components at a given time to be defined.

(ii) A set of modules (appearance, organ growth, development of the pathogen) described the rules driving each component dynamics. Each module integrated the biological rules described in the next section. The time interval for updating the simulation was 1 day. At each time step, rules were applied to each component depending on the accumulated temperature. The structure of the vine stock was recomputed at each time step and the status of the epidemic updated following the update of host growth.

Initial conditions and development of the host

Differences in initial host structure were facilitated by input parameters that reflecting different pruning strategies: height of the trunk, initial number of buds, and distance between buds. First leaves were initiated after reaching a certain sum of degree-days above 10°C (starting on 1 January), varying depending on grape cultivar and date of pruning (Bindi *et al.*, 1997; Gaudillere *et al.*, 1999). For shoot topping, removal of leaves associated with shoots exceeding a given height at a chosen date was simulated.

Leaves and internodes

The model included the appearance and development of both primary and secondary leaves. The initial appearance of leaves on the shoots was controlled by temperature and corresponded to an accumulated sum of 20 degree-days above 10°C (Miglietta *et al.*, 1992; Schultz, 1992). The maximum theoretical size, S_{row} , for a leaf at a given level on a shoot depended on its row on the shoot and on a theoretical maximum leaf surface, S_{max} , thus:

$$S_{row} = \frac{S_{max}}{1 + ae^{(1-row)}} \quad (1)$$

where a was a scaling parameter fitted to the surface of the first leaf, S_1 , thus: $a = (S_{max} - S_1)/S_1$.

Change in the area of leaf surface, S , with time, t , followed a logistic equation of the form

$$\frac{dS}{dt} = \Psi(T)S(1 - \frac{S}{S_{row}}) \quad (2)$$

with a growth-rate-functional response to temperature $\Psi(T)$ (from 0 to 1). Temperature for leaf appearance and S_{max} were input parameters that could be changed depending upon the grape cultivar, whilst parameters could vary for primary and secondary leaves. The length of internodes depended also on temperature and their position on the shoot. The maximum size of internodes followed a logistic growth pattern similar to that of the leaves (Eqn 1).

Secondary shoots

In vineyards, the appearance and growth of secondary shoots is highly variable, depending on the vigour of the vine and the date and extent of shoot topping. The final length of a secondary shoot depends on the position of the shoot on the primary stem and on the dominance (apical) of the primary stem. In this model, the number of leaves on a secondary shoot depended on its row, N , on the primary shoot and was given by a distribution function

$$E[v \cdot N \cdot e^{-kN}] \quad (3)$$

where k was a shape parameter, $1/k$ corresponded to the row at which a secondary shoot achieved the maximum number of leaves, v drove the maximum number of leaves on a secondary shoot and $E[X]$ was the integer part of X .

The development of secondary shoots is stimulated by topping (resulting from the removal of apical dominance in primary shoots), but growth was described in a similar way to that for primary shoots (logistic in type and dependent on temperature), with different parameters (maximum length). The rate of appearance and development of secondary leaves could also be enhanced by a parameter for vigour.

Grape clusters

The precise geometry of grape cluster development was not introduced into the model. Grape clusters were instead represented as simple cones growing over time and located on primary shoots at a level between the second and fifth primary leaf (based on experimental data). Grapes appeared at the same time as primary leaves and their growth followed a rhythm driven by temperature.

Parameters

Parameters related to the appearance and size of leaves and internodes were assessed and estimated from data collected during 2002 from vineyards at INRA Grande Ferrade of cv. Cabernet Sauvignon, after marking and scoring the occurrence of each new leaf on a set of 94 (2002) shoots.

Other parameters, such as angles of growth and leaf orientation were directly included in the computing code and were determined based on 20 digitalized vines.

Pathogen development

Temperature and leaf age are generally recognized as the driving force for pathogen development (growth and sporulation of lesions), whilst wind factors (direction, speed) dictate inoculum (spore) dispersal (Rabbinge & Bastiaans, 1989). In the model presented here, the dynamics of the pathogen population on leaves were split into three key processes: (a) infection, (b) colony or mycelium growth, and (c) sporulation and dispersion. The time between infection and sporulation was described as the latent period, and the duration of sporulation as the infectious period.

The standard formula of Analytis (1977, 1980) was used to describe the effect of temperature on the rate of spore infection and on the rate of mycelium growth. F was a function of a normalized temperature T_n .

$$F(T_n) = \frac{(m+n)^{(m+n)}}{n^n m^m} T_n^n (1-T_n)^m, \text{ with } T_n = \frac{T(t) - T_{\min}}{T_{\max} - T_{\min}}, \quad (4)$$

where $T(t)$ was temperature at time t and T_{\max} and T_{\min} were the cardinal temperatures for either mycelial growth or infection ($T_{\max g}$ and $T_{\min g}$, respectively), with m and n (mg and ng, respectively) shape parameters of the curve. F followed a gamma function with temperature.

Infection

Experimental data relating percentage, I , of spores capable of infecting a leaf of age, A , were described by the function

$$I = I_0 F(T_n) e^{-\tau A} \quad (5)$$

with τ the decay rate of leaf susceptibility, I_0 the maximum infection rate at optimum temperature, and $F(T_n)$ the gamma function with change in temperature T (cf. Eqn 4). $I_0 F(T_n)$ was almost zero at $T < 10^\circ\text{C}$ and $T > 30^\circ\text{C}$; it had a maximum at $T \approx 22^\circ\text{C}$ (Delp, 1954; Sall, 1980).

Colony growth

From experimental data describing the growth of powdery mildew colonies on leaves sampled in the vineyard and contaminated by one spore, the colony diameter, D , over time, t , had a temperature-dependent logistic form. To avoid temperature-driven numerical oscillations in diameter, the discrete linearized form was used:

$$D(t+1) = D(t) + K_{\max} \cdot F(T_n) \cdot \frac{r \cdot e^{r(t^*-t)}}{[1 + e^{r(t^*-t)}]^2} \quad (6)$$

with K_{\max} the maximum colony diameter, r the rate of growth, t^* the time to $K_{\max}/2$, and $F(T_n)$ the rate of mycelium growth with temperature (cf. Eqn 4).

The maximum diameter of the colony also decreased as a function of leaf age

$$K_{\max} = (A - B)e^{(-c \cdot \text{age})} + B \quad (7)$$

where A , B and c were scaling parameters.

Latent period

The latent period represented the time between initial infection and the appearance of new spores. The expected latent period, $\rho(T)$, at temperature T was given by

$$\rho(T) = \frac{\rho_{\min}}{F(T_n)} \quad (8)$$

where ρ_{\min} was the minimum time before the appearance of the first spores (Analytis, 1980; Gessler & Blaise, 1992; Rumbolz, 1999). In the model, the latent period was completed when $\Sigma [1/\rho(T)] = 1$, with $1/\rho(T)$ the fraction of the latent period at temperature T .

Sporulation

The quantity of spores released from a lesion depends on wind speed (Wilocquet *et al.*, 1998). The fraction, Q_s , of spores dispersed from a sporulating leaf at a given wind speed, u ($\text{m} \cdot \text{s}^{-1}$), takes the following form

$$Q_s = \frac{e^{au+b}}{1 + e^{au+b}} \quad (9)$$

with parameters α and b . The quantity of spores, Q , produced during a given period was a function of the colony size, s , thus:

$$Q = \beta e^{(\delta s)} \quad (10)$$

with δ and β scaling parameters.

The quantity of spores released from a colony of a given size at time t was:

$$Q_r = Q_s [Q(t) + R(t-1)] \quad (11)$$

with $R(t-1)$ the quantity of infectious spores not dispersed at time $t-1$.

Infectious period

The sporulation period or infectious period is poorly understood for powdery mildew of grapevine, with reports of it ranging from 3 to 20 days (Chellemi & Marois, 1991; Blaise & Gessler, 1992; Gessler & Blaise, 1992). In this model, the infectious period, one of the most difficult parameters to measure, is accounted for with one input variable.

Inoculum (spore) dispersal

Spore dispersal was described as the motion and short-range dispersal of a large sample of particles released from each source (colony). At each time step, a quantity, Q_r , of spores was released, depending on wind intensity and colony size. These spores were dispersed within a cone of angle θ with respect to an axis given by wind direction. Spore density decreased in two ways, first as an exponential dilution with axial distance to the source, d (with cid a parameter of decay with the distance) and then linearly according to the radial position, $r(\theta)$, within the cone. The quantity of spores deposited on a leaf, Q_c , depended upon its distance from the source, $(d, r(\theta))$, and was proportional to surface area ($Q_c \equiv Q_r S \exp(-cid \cdot d)$) (Fig. 1).

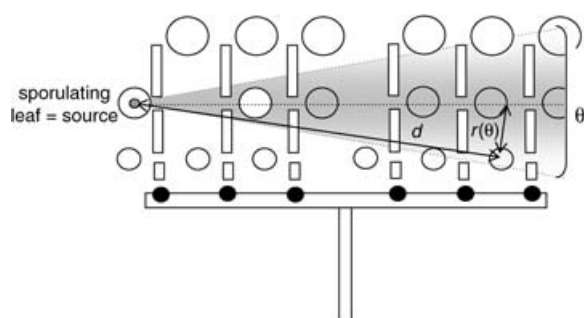


Figure 1 Schematic representation of the dispersal process from a sporulating source. The number of spores deposited on a leaf depends upon its distance, d , from the source, its radial position, $r(\theta)$, in the cone of spores released, and its surface area, S .

Following each time step, the model tracked the x , y , and z coordinates of each group of released and received spores over time. The percentage of spores infecting a leaf of a given age and at a given temperature was determined by Eqn 5. Eddies of wind and leaf shaking are the most efficient for the spore dispersal. Because vertical wind speed was not available from standard climatic data and had to be calculated from hourly climatic data, maximum wind speed and direction for the maximum speed during the day were used instead of the average wind speed.

Parameters

Parameters for pathogen development were assessed from literature (latent period, spore release) or estimated from laboratory experiments carried out at INRA, Bordeaux, from 2001 to 2003 on detached leaves removed from cuttings (infection and colony growth as a function of temperature) or from shoots of field grown vines (sporulation, infection or colony growth, depending on leaf age).

Model output

Outputs of the model described temporal changes over time in:

- Number and location of healthy and infected (latent or infectious) primary and secondary leaves;
- Surface area of healthy, infected and sporulating tissues, with corresponding severity (percentage of area diseased or percentage of area sporulating);
- Number and state of leaves for their corresponding age class; leaves were classified into four susceptibility classes, based on data of ontogenic resistance under controlled conditions: s1, leaves younger than 5 days (highly susceptible); s2, leaves older than 5 and younger than 10 days (susceptible); s3, leaves older than 10 and younger than 20 days (low susceptibility); s4, leaves older than 20 days;
- Number of infectious colonies;
- Total quantity of spores released by the vine and quantity of spores escaping from the vine (i.e. not deposited on leaves or lost to the ground).

Outputs also described the spatial state of the vine stock at each time step, together with all other necessary informa-

tion: coordinates, size, age and disease severity of all plant organs. These outputs were translated by the computer graphics software POV-Ray, providing a representation of the development of the single vine stock over time and its infestation by *E. necator*. The series of images obtained could then be transformed into an animation of annual vine growth (Fig. 2).

The simulator was developed using the high-level programming language C++, an interface making the model available to a wider scientific audience. The exported files were processed by EXCEL macros to provide pertinent epidemiological graphs and were compatible with AMAPMOD (Godin & Caraglio, 1998) to provide users with a supplementary background of statistical tests.

Table 1 and Fig. 3 illustrate all the processes and parameters of host growth and pathogen development included in the model.

Validation of the model

Final leaf surface areas and internode lengths were validated from data of 2002 (Fig. 4). Primary and secondary leaf production were validated by tracking their appearance on a set of 20 shoots during 2003 (Fig. 5a,b,c). A preliminary validation of disease progression was performed by comparing simulated epidemics with disease data from experiments conducted in 2001 (Calonnec *et al.*, 2006). These experiments were performed on three-vine microplots (cv. Cabernet Sauvignon) in which the central vine was artificially inoculated on the central shoot on one of two dates: 4 May (day 124) or 16 May (day 133) corresponding respectively to the three- (L3) and five- (L5) expanded-leaves phenological stages. Inoculation was performed by dispersing spores from two sporulating leaf discs placed at the top of a Cellophane funnel attached around the shoot. Disease incidence and disease severity were assessed on the central vine: 10 primary leaves per shoot, two shoots per vine (30 May, 8 and 18 June and 2 July). Two simulations were performed to reproduce disease data from these artificial inoculations with infections at day 124 on leaves L1 to L3 (sim 124) and at day 133 on leaves L1 to L5 (sim 133). Three variables of interest available from the data were considered: the proportion of primary diseased leaves, the average severity on primary leaves and the relationship between disease incidence and disease severity. Data and simulations were compared by repeated measures analysis of variance.

Model behaviour

Environmental data of 1998 and 2003, reflecting two contrasting yet representative seasons of vine growth (Fig. 6), were used to examine the sensitivity of a leaf epidemic to the date and stage of initial inoculation and to explain differences in epidemic development according to interactions between the development of the host and the pathogen. The year 2003 was characterized by early budbreak, quicker development and high production of secondary shoots because of high temperatures. Simulated

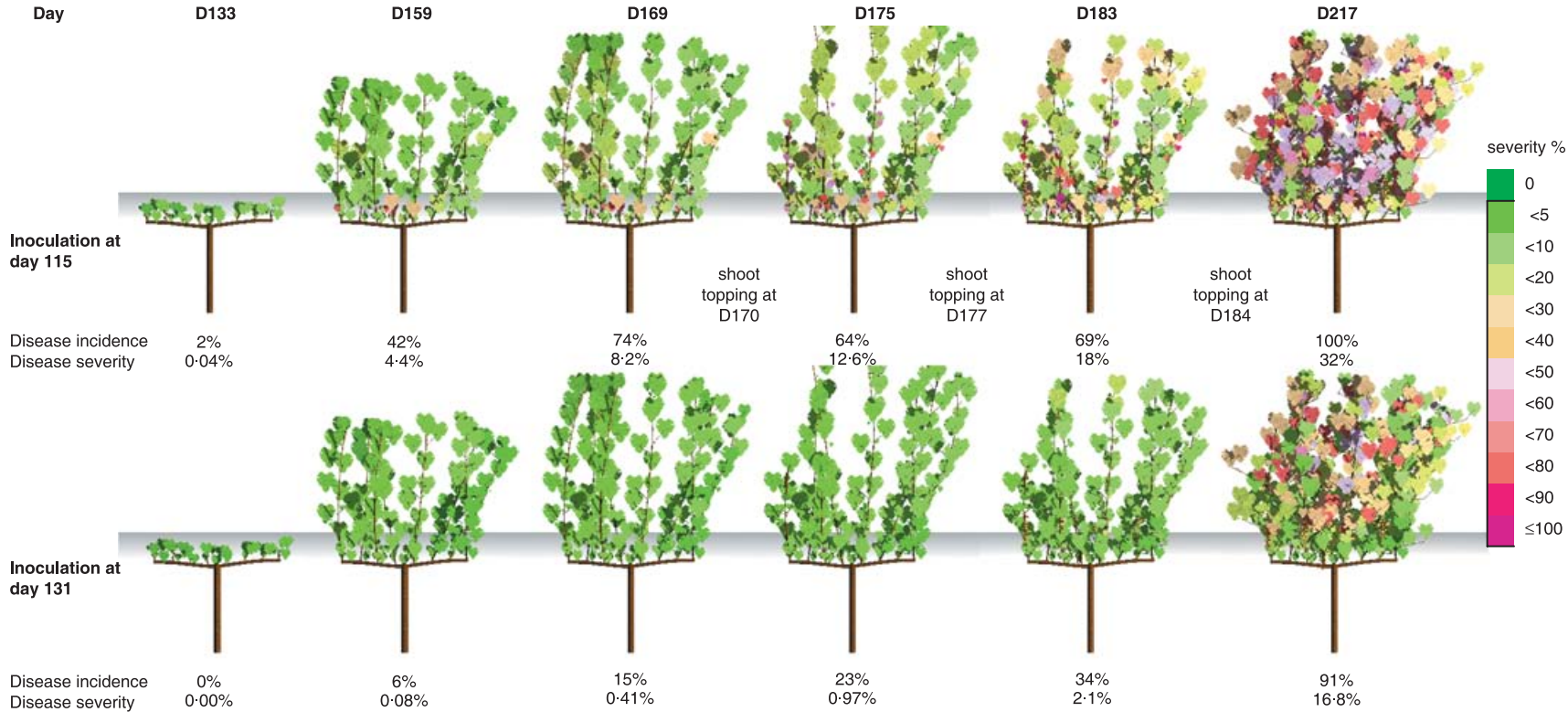


Figure 2 3-D descriptions of the development of a single grapevine stock over time for the year 1998, inoculated with powdery mildew (*Erysiphe necator*) on day 115 or day 131. Shoot topping occurred on day 170. Leaf colour indicates disease severity.

Table 1 Grapevine powdery mildew model parameters

Process	Parameter	Description	Equation no.	Parameterization	Range of value	Units
Initial conditions	h_{trunk}	Height of the trunk		Input	50	cm
	n_{buds}	Number of buds		Input	8	
	d_{buds}	Distance between buds		Input	10	cm
	h_{topping}	Height of topping		Input	150	cm
	t_{topping}	Day of topping		Input	160–170	calendar day
Leaf appearance	v	Drives the maximum number of secondary leaves on a secondary shoot	3	INRA, field measurements	3	
	k	Shape parameter	3	2002–03	0–15	
	$S_{\text{max1}}-S_{\text{max2}}$	Maximum theoretical surface of a primary (max1) or secondary (max2) leaf	1		190–100	cm ²
	$L_{\text{max1}}-L_{\text{max2}}$	Maximum theoretical length of an internode on primary (max1) or secondary shoot (max2)	1		9–6	cm
Spore infection	I_0	Maximum infection rate	5	INRA, controlled inoculations on	0–53	
	τ	Leaf susceptibility decay with age	5	detached leaves	0–147	
	ng, mg	Shape parameter	4	Delp (1954); Sall (1980)	1–055–0–338	
	$T_{\text{maxg}}-T_{\text{ming}}$	Cardinal temperature for pathogen infection	4	Analytis (1977, 1980)	33–5	°C
Colony growth	$n-m$	Shape parameter	4	Analytis (1977, 1980)	1–24–0–27	
	$T_{\text{max}}-T_{\text{min}}$	Cardinal temperature for pathogen growth	4	Analytis (1977, 1980)	33–5	°C
	r	Rate of colony growth	6	INRA, controlled inoculations on	0–2	
	t^*	Time at 50% of growth	6	detached leaves	13	day
	$A-B$	Maximum, minimum colony diameter	7		18–2	mm
	c	Rate of colony growth with the leaves age	7		0–08	
Latent period	p_{min}	Minimum time (in day) for latency	8	Blaise & Gessler (1992); Rumbolz (1999)	6	day
Sporulation	α, b	Parameters in the release function	9	Willoquet <i>et al.</i> (1998)		
	β, δ	Parameters in the spore production function	10	INRA, controlled inoculations on detached leaves	874–0–314	
Dispersion process	cid	Spore decay with distance			0–04	
Infectious period	DI	Duration of infectious period in days		Input	10	day

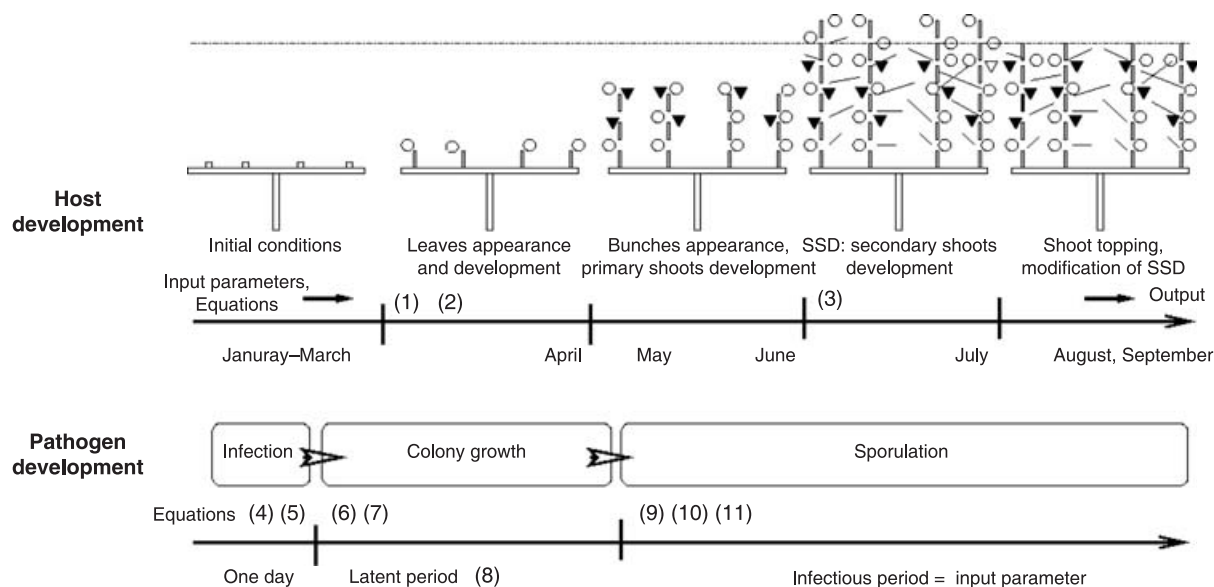


Figure 3 Schematic representation of host grapevine growth during a season and of pathogen (*Erysiphe necator*) development during an infection cycle, implemented in the model. Numbers refer to equations in the text.

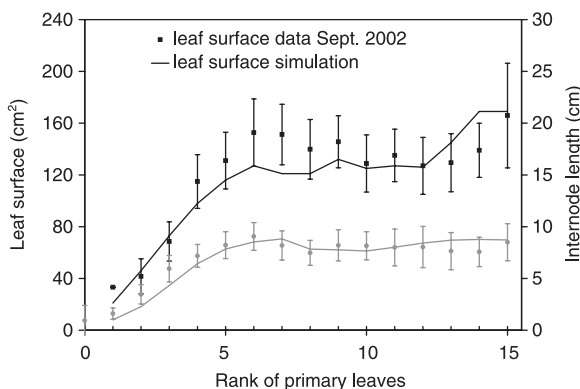


Figure 4 Variation of the average grapevine leaf area and internode length as a function of row number on a primary shoot for the year 2002.

epidemics were initiated by considering the infection of the first expanded leaf (the closest to the bark) at different phenological stages (from stage-1 to stage-7 expanded leaves; L1–L7) of vine development. For these simulations, the day of flowering, when grape bunches were at their most susceptible to the disease, was achieved when the accumulated sum of the mean daily temperature above 10°C reached 380 starting from day 1 (1 January). Shoot topping was simulated 10 days after flowering. Parameters used for simulation are summarized in Table 1. In these simulations, for two contrasting growing seasons, 1998 and 2003, (i) the sensitivity of epidemic development to the time of first infection was examined with particular emphasis on disease severity at time of flowering, (ii) a direct comparison of epidemic behaviour was made for the two contrasting growing seasons from the same day of initial infection, (iii) differences in epidemic development were examined according to changes in susceptibility classes of the leaf population and (iv) the relationship between rate of disease development and relative volumes of sporulating and susceptible leaf tissue was investigated.

Results

Model validation for temporal disease progression

Data describing changes in the proportion of primary leaves diseased over time were highly variable, with a higher standard deviation for vines inoculated on day 124 than for those inoculated on day 133 (Fig. 7). Simulations were remarkably consistent with experimental data, showing the same trends and with no significant differences for the three variables of interest: proportion of primary diseased leaves (data 124 vs. sim 124, $P = 0.81$, interaction $P = 0.47$; data 133 vs. sim 133, $P = 0.91$, interaction $P = 0.88$), average disease severity (data 124 vs. sim 124, $P = 0.74$, interaction $P = 0.97$; data 133 vs. sim 133, $P = 0.35$, interaction $P = 0.50$) and the relationship between the two hierarchical scales (disease incidence vs. disease severity) (Fig. 7). There was, however, a closer

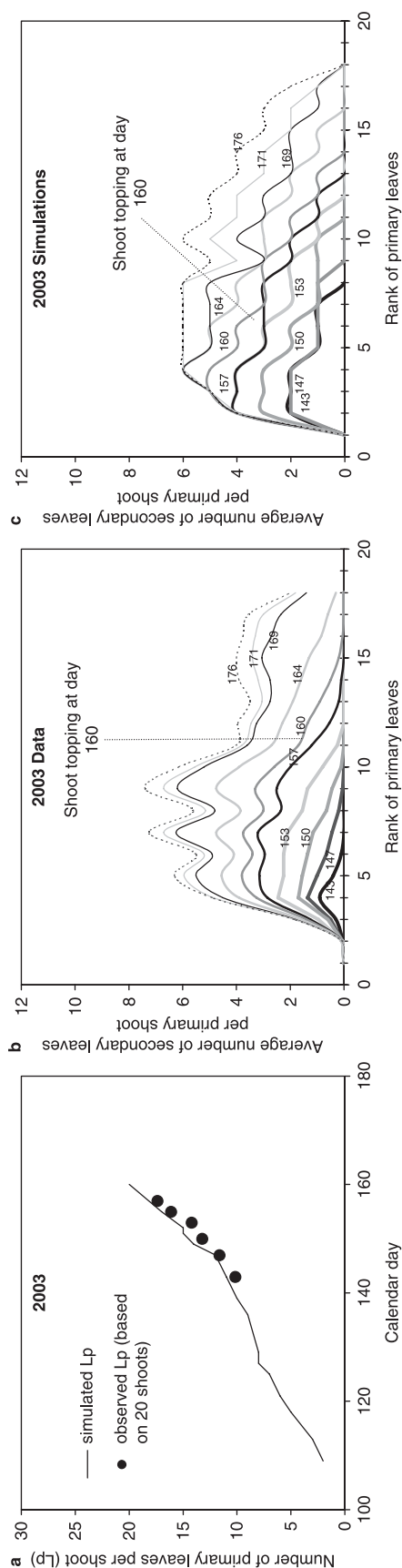


Figure 5 Results of grapevine host development for the year 2003. (a) Comparison of observed and simulated numbers of primary leaves per shoot over time. (b) Observed and (c) simulated evolution of the average number of secondary leaves per primary shoot rank, from day 143 to day 176.

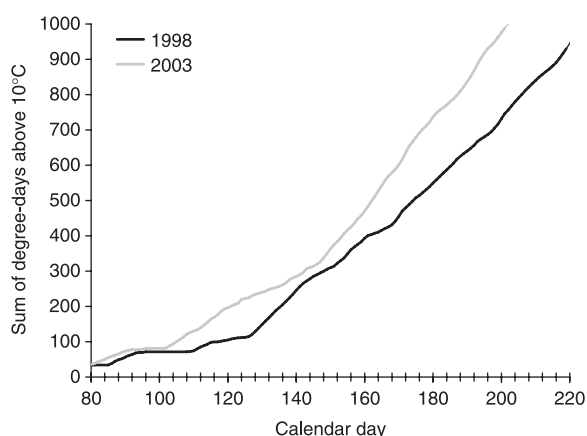


Figure 6 Comparison of the sum of degree days above 10°C for the years 1998 and 2003 (climatic data for Cadaujac, 3 km south of Bordeaux).

relationship for the later inoculation date. For both experimental data and simulations, an effect of the date of primary inoculation resulted in a delay in epidemic development of about 12 days and a significant difference in disease severity on primary leaves.

Effects of date of primary inoculation and of host development on disease progress

Epidemics simulated using environmental data from 1998 and 2003 were characterized by increasing disease progression on primary leaves until the time of the second shoot topping (day 177 for 1998 and day 167 for 2003) (Fig. 8a,b) and lengthened on secondary leaves (Fig. 8c,d). For early inoculation (at phenological stage L1–L3), the rate of initial disease progress on primary leaves followed the rate of leaf production, with a delay of approximately 18 days (1998) or 28 days (2003) (Fig. 8c,d). For 1998, disease was most severe for an epidemic initiated at the first leaf stage (day 115) (Fig. 8a,c). In relation to the critical time for berry infection (day 159, corresponding to flowering) a significant reduction in the proportion of diseased leaves, from 42% when inoculated at stage L1 (day 115) to 23% at L2 (day 123) and L3 (day 129), and to 6% at L4 (day 131), was detected (Fig. 8e). Stimulated by differences in climatic variables, vine development in 2003 was characterized by budbreak 10 days earlier than for 1998, a higher rate of initial primary leaf development and a higher rate of development of secondary leaves after day 160. For 2003 data, disease severity at flowering (day 152) was similar when inoculation occurred at either L1 (day 105) or L2 (day 108) (24% of total leaves diseased) and decreased when initial infection was delayed to L3 or L4 (days 111 and 115, respectively; 9% of leaves diseased) and further still when delayed to L5–L7 (days 117–124; 1% of leaves diseased) (Fig. 8b,d,f). Depending on the date of initial contamination, these differences could result in the 1998 epidemic being characterized by higher levels of disease than the 2003 epidemic at around the time of

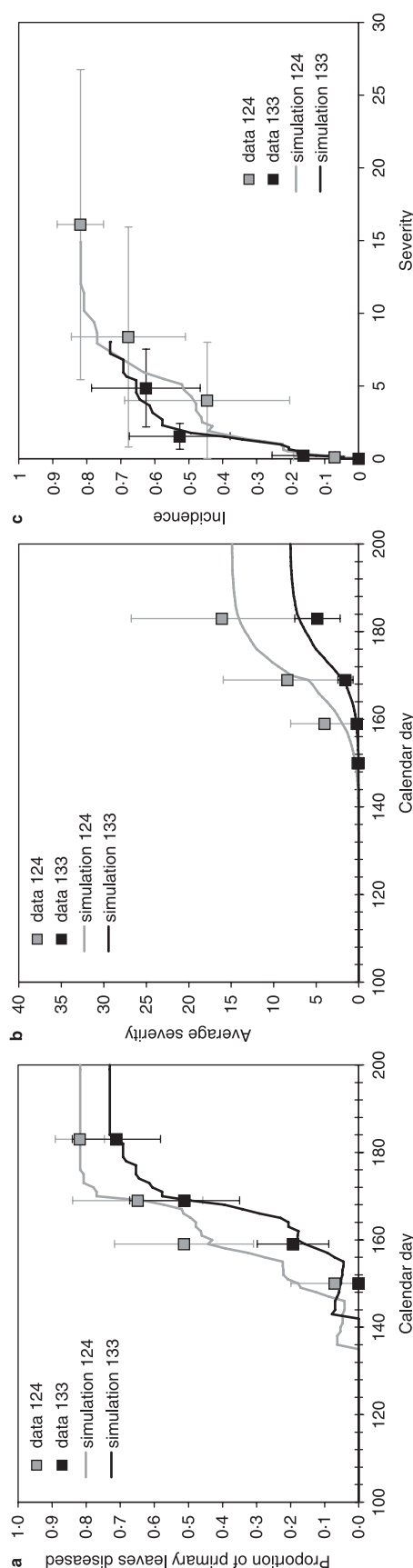


Figure 7 Comparison of experimental data (squares) with model simulations (continuous lines) for grapevine powdery mildew for the year 2001, for three variables: the proportion of diseased primary leaves, the average severity for diseased primary leaves and the incidence vs. severity for diseased primary leaves. Inoculations were performed on day 124 on first to third leaves (grey) and on day 133 on first to fifth leaves (black). Bars indicate the standard deviation of the mean for experimental data.

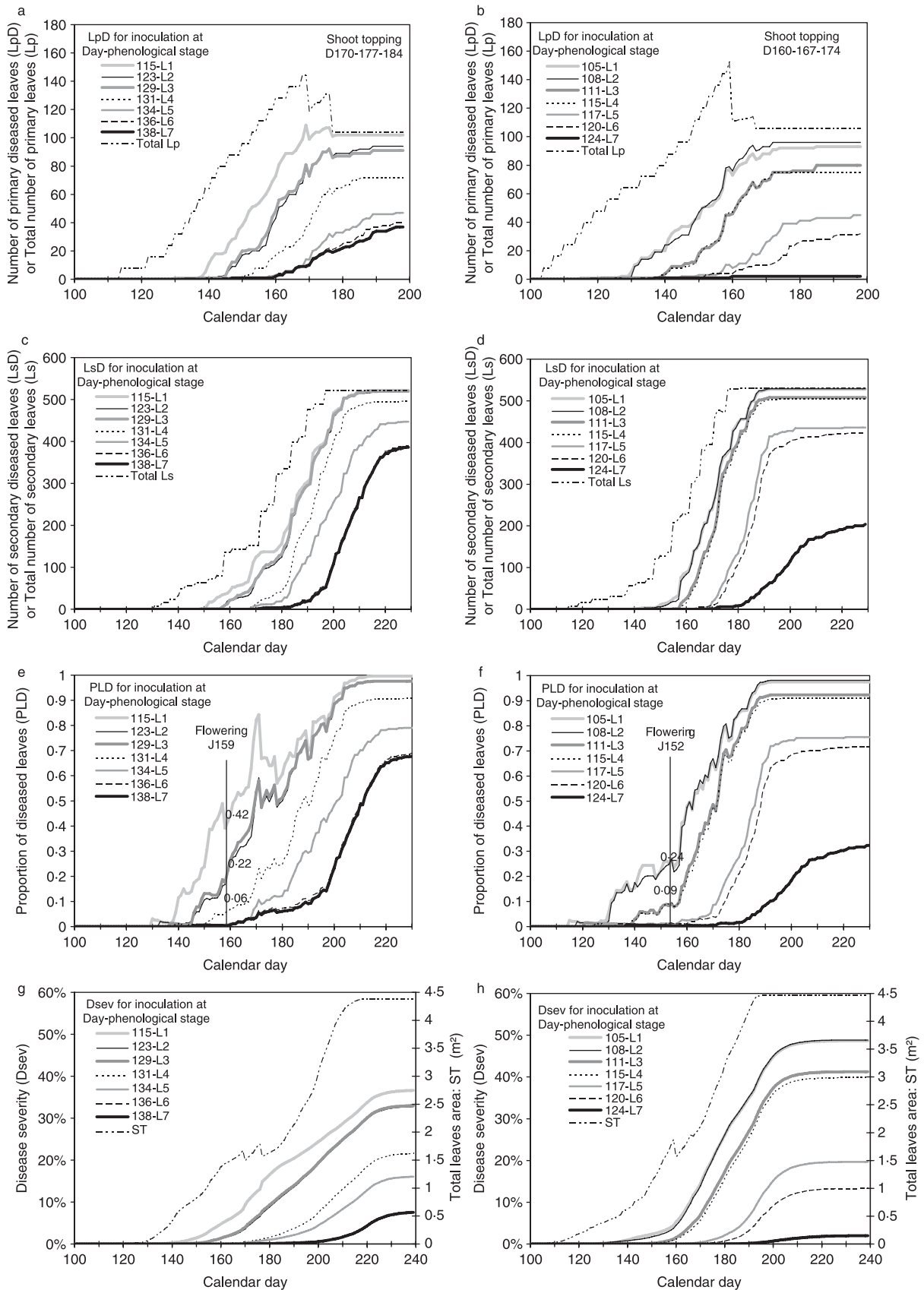


Table 2 Initial conditions for 1998 and 2003 grapevine powdery mildew simulations

Year	Condition at inoculation	Conditions at beginning of first sporulation event			Average percentage susceptible leaves during spo1	Number of spores captured during spo1	Number of infected leaves during spo1
	Stage ^a /Day	Phenological stage ^a	Length of shoots (cm)	spo1 ^b days			
1998	1L/115	L4	2.2	130–137	75.4	4493	32
	2L/123	L5	5.2	133–142	73.6	6553	22
	3L/129	L7	12.0	137–144	72.9	3234	24
	4L/131	L8	17.0	139–148	64.3	3227	22
	5L/134	L9	27.0	142–151	55.4	3210	12
	6L/136	L10	32.3	144–153	47.7	3720	19
	7L/138	L11	39.8	147–158	37.9	4246	14
2003	1L/105	L4	3.3	115–123	72.8	1502	19
	2L/108	L5	7.1	119–128	63.3	3671	26
	3L/111	L6	8.6	121–130	53.5	1609	13
	4L/115	L7	13.8	125–134	40.9	3043	12
	5L/117	L8	17.4	128–137	32.9	2107	3
	6L/120	L9	23.7	133–142	32.9	4625	6
	7L/124	L9	29.8	137–146	36.2	2524	3

^aNumber of expanded leaves.^bspo1 = first sporulation event.

flowering (incidence and severity), but with lower final levels of disease.

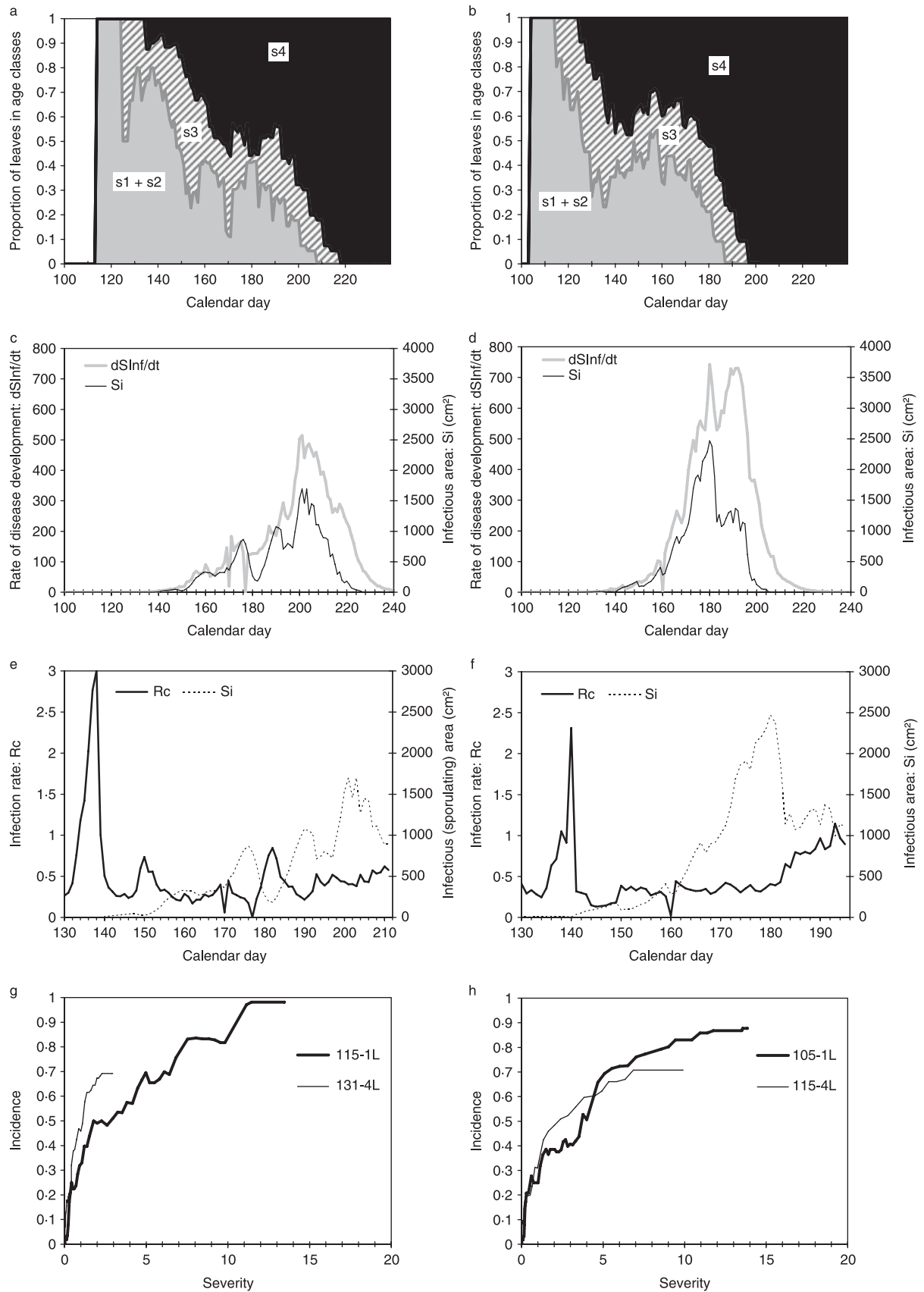
When comparing the same dates of initial infection across the two different growing seasons, differences in epidemic behaviour were enhanced. For primary infections occurring at day 115, a vine with late budbreak (such as in 1998) could show 58% of primary leaves diseased at flowering compared with only 19% for a vine with early budbreak (such as in the 2003 season) (data not shown). In contrast, for early primary infection at day 105 and with only one ascospore release event, the year 1998 (or a variety having a late budbreak) could escape the epidemic. Decrease in disease severity with a delay in the date of first infection was higher for 2003 than for 1998 (Fig. 8g,h). Shoot topping had an effect in decreasing disease severity in 1998, but not in 2003.

In both years, growth of the vine was characterized by a progressive change from a leaf population of age classes corresponding to highly susceptible leaves ($s1 \leq 5$ days old) to a leaf population of age classes corresponding to lower susceptibility to disease (Fig. 9). For 2003, the percentages of highly susceptible leaves ($s1 + s2$) decreased rapidly at the beginning of the season (until day 135) and increased again with the development of secondary leaves until day 155 and then decreased to zero after 190 days. For 1998, the overall decrease in the most susceptible classes was less rapid, declining to zero after approximately 210 days. When the early stage of the epidemic was considered, the average percentage of infected leaves

during the first sporulation event was positively and linearly correlated with the percentage of susceptible leaves ($s1 + s2$) present during this period (for 1998, $R^2 = 0.60$, $P = 0.04$; for 2003, $R^2 = 0.76$, $P = 0.008$) (Table 2). Furthermore, the number of leaves infected at the first sporulation event was negatively correlated with the length of the shoot at the stage of the first sporulation event (Table 2). The sensitivity of these leaf epidemics to the stage of initial inoculation could result in a dilution of susceptible leaves ($s1 + s2$) with older leaves, combined with an increase in distance between primary infected leaves and these susceptible leaves.

The rate of disease development (dS_{Inf}/dt) corresponding to the variation with time of infected area (S_{Inf} = latent + sporulating) was proportional to the variation of infectious (sporulating) area (S_i), in accordance with Van der Plank's equation $dS_{Inf}/dt = R_c \cdot S_i \cdot (1 - S_{Inf}/ST)$ (Fig. 9c,d). Furthermore, the rate of disease development decreased in accordance with a logistic growth of the disease, at the time when 50% of the maximum infected area was reached. As a result of ontogenic resistance only 36% (1998) to 48% (2003) of the total area was diseased. From the variation of infected area (S_{Inf}), the sporulating area (S_i) and the total area available for contamination (ST), the infection rate (R_c) was calculated at each time step (Fig. 9e,f). The last ST considered corresponded to the total leaf surface until about 15 days after emergence of the last leaf (end of leaves surface extension). Infection rate showed some variations: a

Figure 8 Evolution over time of (a, b) the number of diseased primary and (c, d) secondary leaves, (e, f) the proportion of diseased leaves or (g, h) the mean severity of disease on individual leaves for several grapevine phenological stages and times of primary inoculation (one to seven expanded leaves; L1–L7) with powdery mildew (*Erysiphe necator*) and two sets of environmental data (1998 and 2003). (a, c, e, g) Simulations for 1998; (b, d, f, h) simulations for 2003. Inoculation was on the first primary leaf.



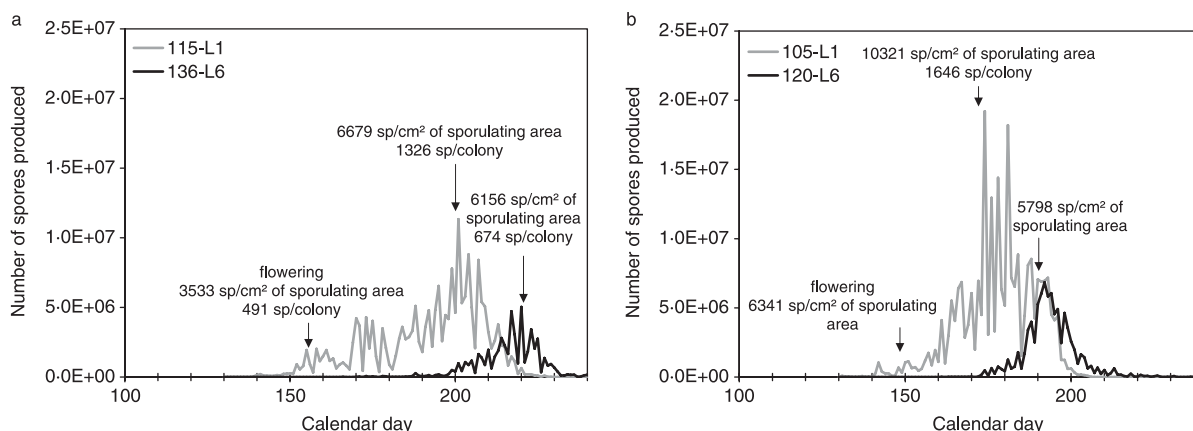


Figure 10 Evolution over time of the proportion of *Erysiphe necator* spores produced per grapevine stock. Simulation based on environmental data of (a) 1998 and (b) 2003 for two dates of primary infection (days 115–136 for 1998 and 105–120 for 2003).

reduction after shoot topping, especially for 1998, and an increase linked to development of secondary leaves after day 180 for the year 2003. The relationship between disease incidence and disease severity, when considering primary leaves, was similar to that observed in 2001, with about 15% severity for approx. 90–100% of diseased leaves (Fig. 8g,h). Dispersion was less for the first part of the epidemic in 2003 (more aggregation), probably because of a higher rate of shoot development. Sporulation profiles were different for 1998 and 2003, following the trend of sporulating areas, with a delayed major peak of sporulation and a decreased total amount of sporulation for delayed inoculation (Fig. 10a,b). The number of spores released per area of sporulating tissue was on average around 5000 spores cm^{-2} .

Discussion

The objective of this work was to build a simulation model combining growth of the vine plant with the development of a powdery mildew epidemic, providing a tool with which to examine the dynamic interactions between pathogen, host and environment, which together account for variability in epidemic behaviour and the capacity of host development to modify disease progress. The model developed had several advantages over other existing models. It accounted for key pathogen, host and environmental parameters that determine the spread of plant disease. In particular, the rate of production, location and phenological status of the host (leaf) population, together with the dispersal process and parameters specific to the development and spread of the pathogen, were included. Considering these parameters and their control together, the model allowed their interactions to be analysed. Moreover, where many models assume synchronous

initiation of host and pathogen growth, this model allowed different times for the initiation of host growth and pathogen infection, together with periodic changes resulting from host development forced by crop management (shoot topping and vigour). The model also enabled the impact on epidemic development of real sets of climatic data, corresponding to known and contrasting scenarios for crop development, to be tested.

For a given set of environmental inputs, the model output was remarkably consistent both with epidemiological field data (Fig. 7) and with the output from other theoretical analytical models (Van der Plank, 1963). Particularly notable was the consistency of model output with the ratio of disease incidence to disease severity for epidemics initiated at different times. This suggested a high degree of accuracy for the host growth and epidemiological parameters used in the model, affecting the appearance and expansion of leaves and fungal colonies. Simulations also suggested that the spread of disease is sensitive to changes in host growth, host phenology and host susceptibility, and to parameters that affect the specificity of the viticultural production system.

In this paper, a relatively simple but very important example was used to demonstrate the potential of the model for use as a research tool. By considering epidemic behaviour in response to a characteristic feature of powdery mildew epidemics, namely, contrasting environmental regimes that lead to early or late budbreak, the model was used to understand the link between the timing of initial contamination and disease severity at flowering. Given that the disease severity on leaves represents the inoculum load for grape infection, this difference has significant implications for grape damage (Calonne *et al.*, 2006). The results of these initial simulations showed that the severity of a leaf epidemic at the time when grape bunches

Figure 9 Evolution over time of (a, b) grapevine leaves in age classes according to simulation, (c, d) rate of *Erysiphe necator* disease development and infectious area, (e, f) infection rate and (g, h) incidence vs. severity relationship for two dates of inoculation. (a, c, e, g) Simulations for 1998; (b, d, f, h) simulations for 2003. S1 + S2 = leaves up to 10 days old; S3 = leaves older than 10 and younger than 20 days; S4 = leaves older than 20 days.

are most sensitive to powdery mildew was conditional upon two key factors: (i) the timing of the first sporulation event, upon which, in turn, depended the time of initial infection and the length of the latent period thereafter, and (ii) the availability (number, location and susceptibility) of susceptible leaves during this period. Moreover, the results pointed to a high degree of nonlinearity in the system whereby small changes in the onset of an epidemic can, as a consequence of changes in leaf susceptibility and of their position in the leaf canopy, have profound consequences for the severity of an epidemic later in the season (Xu & Ridout, 1998). This dynamically generated variability (Kleczkowski *et al.*, 1996) was demonstrated previously for soilborne plant pathogens, in which small differences early in an epidemic, combined with the non-linear, multiplicative effects of secondary infection and dynamic changes in host susceptibility, can lead to large differences in final levels of disease. Increased host development, later in the season, may also increase final levels of disease and disease severity. Whilst late disease development may be of no consequence in terms of the damage caused to grape bunches, it may affect the amount of chasmothecia formed and consequently the quantity of primary inoculum in the next year. In contrast to the results of simulations performed by Gessler & Blaise (1992), an increase in host growth (secondary leaves) at the time at which the rate of disease development began to decrease did not slow the epidemic in the present model. As soon as new susceptible leaves were produced, the rate of disease development increased. The simulations suggested that infection rate may also decrease after shoot topping. This was no doubt the result of the loss of sporulating leaf area, especially pronounced for the 1998 epidemic.

It is suggested that, by using this model to better understand the dynamic interactions between pathogen, host and environment, the variability that develops within and between epidemics can be both accounted for and exploited (for better disease management) by, for example, the use of phenological status as a disease risk indicator, the deployment of control agents, the management of the training system or the selection of varietal traits that delay the first sporulation event beyond the critical time of high leaf susceptibility. However, the model did not take into account the potential effect of a reduction in host development as a result of water stress. In such conditions, an increase in temperature later in the season may be not followed by an increase in host development (Garcia de Cortazar Atauri, 2007).

Two key areas for model development are considered: (i) the introduction of variability in budbreak and bunch development and (ii) integration of the model as a sub-model for simulations on a larger plot or field scale. This study gave particular emphasis to the status of the leaf epidemic at the time when the grape cluster was most susceptible to the presence of mildew inoculum, yet the susceptibility of a grape cluster also depends on its phenological age (Gadoury *et al.*, 2003), providing still more scope for nonlinear behaviour within this system. In

the simplest form, berry clusters might be considered as homogeneous units that behave in an identical manner. In reality, the berry cluster is a complex organ with heterogeneous development within and between clusters (Gadoury *et al.*, 2006), leading to equally high levels of heterogeneity in susceptibility to powdery mildew and affecting the impact of the leaf epidemic on the severity of the disease on the berries. To take this into account, it is proposed that a submodel be developed to consider the development of berry structure in space together with changes and variability in phenological status.

The model developed here accounted for the spread of disease within a single vine plant, yet powdery mildew is capable of travelling over considerable distances (Jarvis *et al.*, 2002). The influence of the epidemic at the plant level on the spread of the epidemic at the field level is of considerable interest. For example, are the factors that most affect the local spread of disease (within a plant) the same factors that are largely responsible for the wide-scale (field-scale) dynamics of the epidemic? Consequently, the model at the vine-stock level is being integrated into a model describing disease dynamics at the plot level (Calonnec *et al.*, 2005). At this scale two modes of disease transmission can be considered, short-distance spore transmission described by a ray model, and long-distance spore transmission using a normal distribution model (Bache, 1979; Slinn, 1982). Expansion of a pathogen population in space and time is then modelled by combining the model for the local increase of individuals (spores) with a model for the dispersal of these individuals to new sites (Aylor & Flesch, 2003). In parallel, mathematical models are also being developed to study more precisely the dispersion process on a larger scale (Burie *et al.*, 2006, 2007).

Experimentation to examine other epidemiological components of the system is ongoing, in particular, to improve the accuracy of the model via a better understanding of the roles of leaf infectivity, grape cluster susceptibility and secondary leaf production. Whilst the role of leaf age on leaf susceptibility and hence the probability of infection has been considered, the model will be extended to include the influence of vine management and vine vigour on leaf susceptibility.

Acknowledgements

We thank Y. Brunet (INRA, Ephyse) for his assistance and comments concerning wind dispersion and J. Roman and G. Tessier (LaBRI and INRIA Futurs) for their important contributions on computing. This work was funded by the INRA department of Santé des Plantes, by the French Ministry of Agriculture and Research, and by the region Aquitaine.

References

- Analytis S, 1977. Über die Relation zwischen biologischer Entwicklung und Temperatur bei phytopathogenen Pilzen. *Phytopathologische Zeitschrift* **90**, 64–76.

- Analytis S, 1980. Obtaining of sub-models for modeling the entire life cycle of a pathogen. *Journal of Plant Diseases and Protection* **87**, 371–82.
- Aylor D, Flesch T, 2003. Spread of plant disease on a continental scale: role of aerial dispersal of pathogens. *Ecology* **84**, 1989–97.
- Bache D, 1979. Particle transport within plant canopies. I. A framework for analysis. *Atmospheric Environment* **13**, 1257–62.
- Bindi M, Miglietta F, Gozzini B, Orlandini S, Seghi L, 1997. A simple model for simulation and development in grapevine (*Vitis vinifera* L.). I. Model description. *Vitis* **2**, 67–71.
- Birch CJ, Andrieu B, Fournier C, Vos J, Room P, 2003. Modelling kinetics of plant canopy architecture: concepts and applications. *European Journal of Agronomy* **19**, 519–33.
- Blaise P, Gessler C, 1992. An extended progeny/parent ratio model. I. Theoretical development. *Journal of Phytopathology* **134**, 39–52.
- Burie J-B, Calonnec A, Ducrot A, 2006. Singular perturbation analysis of travelling waves for a model in phytopathology. *Mathematical Modelling of Natural Phenomena* **1**, 1–15.
- Burie J-B, Calonnec A, Langlais M, 2007. Modeling of the invasion of a fungal disease over a vineyard. In: Deutsch A, Bravo de la Parra R, de Boer RJ *et al.*, eds. *Mathematical Modeling of Biological Systems, Volume II. Series: Modeling and Simulation in Science, Engineering and Technology*. Boston, MA, USA: Springer, 11–21.
- Calonnec A, Latu G, Naulin J-M, Roman J, Tessier G, 2005. Parallel simulation of the propagation of powdery mildew in a vineyard. *Computer Science* **3648**, 1254–64.
- Calonnec A, Cartolaro P, Deliere L, Chadoeuf J, 2006. Powdery mildew on grapevine: the date of primary contamination affects disease development on leaves and damage on grape. *IOBC/WPRS Bulletin* **29**(11), 67–73.
- Chellemi D, Marois J, 1991. Sporulation of *Uncinula necator* on grape leaves as influenced by temperature and cultivar. *Journal of Phytopathology* **8**, 197–201.
- Cortesi P, Gadoury DM, Seem RC, Pearson RC, 1995. Distribution and retention of cleistothecia of *Uncinula necator* on the bark of grapevines. *Plant Disease* **79**, 15–9.
- Delp C, 1954. Effect of temperature and humidity on the grape powdery mildew fungus. *Phytopathology* **44**, 615–26.
- Deussen O, Linterman B, 1997. A modeling method and user interface for creating plants. In: Moller T, Ware C, eds. *Graphics Interface Proceedings 1997*. Wellesley, MA, USA: AK Peters Ltd, 189–97.
- Diestel R, 2000. *Graph Theory*. New York, USA: Springer-Verlag.
- Doster MA, Schnathorst WC, 1985. Effects of leaf maturity and cultivar resistance on development of the powdery mildew fungus on grapevines. *Phytopathology* **75**, 318–21.
- Fanizza G, Colonna G, 1996. A mathematical function to study berry growth variability in grapes (*Vitis vinifera*). *Journal of Wine Research* **2**, 117–23.
- Ficke A, Gadoury DM, Seem RC, 2002. Ontogenic resistance and plant disease management: a case study of grape powdery mildew. *Phytopathology* **92**, 671–5.
- Ficke A, Gadoury D, Seem R, Dry I, 2003. Effects of ontogenic resistance upon establishment and growth of *Uncinula necator* on grape berries. *Phytopathology* **93**, 556–63.
- Gadoury D, Seem R, Ficke A, Wilcox W, 2003. Ontogenic resistance to powdery mildew in grape berries. *Phytopathology* **93**, 547–55.
- Gadoury DM, Seem RC, Wilcox WF *et al.*, 2006. Modeling and mapping the relationship between climate and ontogenic resistance to the major fungal diseases of grapevine. In: *Proceedings of the 5th International Workshop on Grapevine Downy and Powdery Mildew*, 157–9.
- Garcia De Cortazar Auri I, 2007. *Adaptation du Modèle STICS à la Vigne (Vitis vinifera L.). Utilisation dans le Cadre d'une Étude d'Impact du Changement Climatique à l'Échelle de la France*. Montpellier, France: ENSAM, PhD Thesis.
- Gaudillere J, Dayau S, Guimberteau G, 1999. Effets des facteurs de l'environnement sur le développement de la vigne. Relations avec l'effet terroir. In: *Actes du Colloque, 5. ème Journée Technique du CIVB, Bordeaux, 1999*, 24–32.
- Gessler C, Blaise P, 1992. An extended progeny/parent ratio model. II. Application to experimental data. *Journal of Phytopathology* **134**, 53–62.
- Godin C, Caraglio Y, 1998. A multiscale model of plant topological structures. *Journal of Theoretical Biology* **191**, 1–46.
- Hanan J, Prusinkiewicz P, Zalucki M, Skirvin D, 2002. Simulation of insect movement with respect to plant architecture and morphogenesis. *Computers and Electronics in Agriculture* **35**, 255–69.
- Hau B, 1990. Analytic models of plant disease in a changing environment. *Annual Review of Phytopathology* **28**, 221–45.
- Jarvis WR, Gubler WD, Grove GG, 2002. Epidemiology of Powdery Mildews in Agricultural Pathosystems. In: Bélanger RR, Bushnell WR, Dik AJ, Carver TLW, eds. *The Powdery Mildews. A Comprehensive Treatise*. St Paul, MN, USA: APS Press, 169–99.
- Kleczkowski A, Bailey DJ, Gilligan CA, 1996. Dynamically generated variability in plant pathogen systems with biological control. *Proceedings of the Royal Society of London Series B – Biological Sciences* **263**, 777–83.
- Miglietta F, Gozzini B, Orlandini S, 1992. Simulation of leaf appearance in grapevine. *Viticultural and Enological Science* **47**, 41–5.
- Peyrard N, Calonnec A, Bonnot F, Chadoeuf J, 2005. Explorer un jeu de données sur grille par tests de permutation. *Revue de Statistique Appliquée* **53**, 59–78.
- Prusinkiewicz P, 1997. In search of the right abstraction: the synergie between art, science, and information technology in the modeling of natural phenomena. In: Sommerer C, Mignonneau L, eds. *Art @Science*. Vienna, Austria: Springer-Verlag.
- Rabbinge R, Bastiaans L, 1989. Combination models, crop growth and pests and diseases. In: Rabbinge R, Ward SA, Van Laar HH, eds. *Simulation and Systems Management in Crop Protection*. Wageningen, Netherlands: PUDOC: Simulation Monographs **32**, 217–39.
- Room P, Hanan J, Prusinkiewicz P, 1996. Virtual plants: new perspectives for ecologists, pathologists and agricultural scientists. *Trends in Plant Science* **1**, 33–9.
- Rumbolz J, 1999. *Untersuchungen zur Konidienkeimung und Mycelentwicklung des Echten Mehltaus der Weinrebe (Uncinula necator (Scw.) Burr.) und deren Einfluß auf die Epidemiologie*. Konstanz, Germany: Universität Konstanz, Dissertation.
- Sall M, 1980. Epidemiology of grape powdery mildew: a model. *Phytopathology* **70**, 338–42.

- Sall M, Wrynski J, 1982. Perennation of powdery mildew in buds of grapevines. *Plant Disease* **66**, 678–9.
- Schultz H, 1992. An empirical model for the simulation of leaf appearance and leaf area development of primary shoots of several grapevine (*Vitis vinifera* L.) canopy-systems. *Scientia Horticulturae* **52**, 179–200.
- Skirvin DJ, 2006. Virtual plant models of predatory mite movement in complex plant canopies. *Ecological Modelling* **171**, 301–13.
- Slinn W, 1982. Predictions for particle deposition to vegetative canopies. *Atmospheric Environment* **166**, 1785–94.
- Tardieu F, 2003. Virtual plants: modelling as a tool for the genomics of tolerance to water deficit. *Trends in Plant Science* **8**, 9–14.
- Tessier G, Roman J, Latu G, 2006. Hybrid MPI-thread implementation on a cluster of SMP nodes of a parallel simulator for the propagation of powdery mildew in a vineyard. *Lecture Notes in Computer Science* **4208**, 833–42.
- Van Der Plank J, 1963. *Plant Diseases: Epidemic and Control*. New York, USA: Academic Press.
- Van Der Plank J, 1982. *Host-Pathogen Interactions in Plant Disease*. New York, USA: Academic Press.
- Weber J, Penn J, 1995. Creation and rendering of realistic trees. In: *Proceedings of SIGGRAPH*, 1995. 119–28.
- West D, 1995. *Introduction to Graph Theory*. Upper Saddle River, NJ, USA: Prentice Hall.
- Willoquet L, Berud F, Raoux L, Clerjeau M, 1998. Effects of wind, relative humidity, leaf movement and colony age on dispersal of conidia of *Uncinula necator*, causal agent of grape powdery mildew. *Plant Pathology* **47**, 234–42.
- Wilson PA, Chakraborty S, 1998. The virtual plant: a new tool for the study and management of plant diseases. *Crop Protection* **17**, 231–9.
- Xu X-M, Ridout M, 1998. Effects of initial epidemic conditions, sporulation rate, and spore dispersal gradient on the spatio-temporal dynamics of plant disease epidemics. *Phytopathology* **88**, 1000–12.